ACS POLYMERS Au
AN OPEN ACCESS JOURNAL OF THE AMERICAN CHEMICAL SOCIETY

pubs.acs.org/polymerau
Article

Discrete Miktoarm Star Block Copolymers with Tailored Molecular Architecture

Published as part of the ACS Polymers Au virtual special issue "2023 Rising Stars".

Zhuang Ma, Zhongguo Liu, Tianyu Zheng, Zhanhui Gan, Rui Tan,* and Xue-Hui Dong*

Cite This: *ACS Polym. Au* 2023, 3, 457−465
Read Online

ACCESS | Metrics & More | Article Recommendations | Supporting Information

ABSTRACT: Molecular architecture is a critical factor in regulating phase behaviors of the block copolymer and prompting the formation of unconventional nanostructures. This work meticulously designed a library of isomeric miktoarm star polymers with an architectural evolution from the linear-branched block copolymer to the miktoarm star block copolymer and to the star-like block copolymer (i.e., 3AB → 3(AB$_1$)B$_2$ → 3(AB)). All of the polymers have precise chemical composition and uniform chain length, eliminating inherent molecular uncertainties such as chain length distribution or architectural defects. The self-assembly behaviors were systematically studied and compared. Gradually increasing the relative length of the branched B$_1$ block regulates the ratio between the bridge and loop configuration and effectively releases packing frustration in the formation of the spherical or cylindrical structures, leading to a substantial deflection of phase boundaries. Complex structures, such as Frank−Kasper phases, were captured at a surprisingly higher volume fraction. Rationally regulating the molecular architecture offers rich possibilities to tune the packing symmetry of block copolymers.

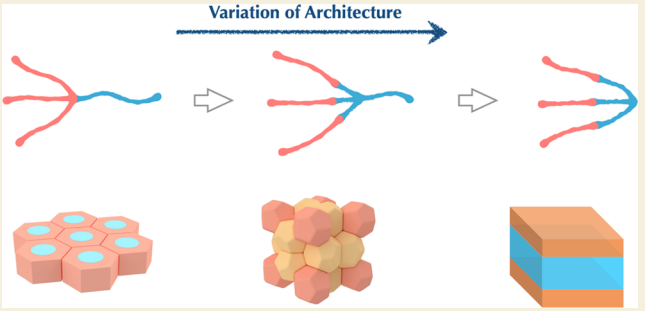

KEYWORDS: *Miktoarm star block copolymer, discrete polymer, architecture, self-assembly, Frank−Kasper phase*

INTRODUCTION

Block copolymers comprised of chemically incompatible chains can spontaneously form a diverse array of ordered nanostructures, with a generic phase progression from lamellae (LAM) to double gyroids (DG), hexagonally packed cylinders (HEX), and body-centered cubic (BCC)-packed spheres as composition becomes increasingly asymmetric.[1−3] It has long been recognized that the simplest AB linear diblock copolymers having similar Kuhn segment length (b) usually exhibit a symmetric phase diagram with respect to volume fraction, and the self-assembly behaviors depend mainly on three molecular variables: overall chain length (N), volume fraction (f), and Flory−Huggins interaction parameter (χ).[4] Molecular architecture, on the other hand, has been proven to be another important factor to deflect the phase diagram and prompt the formation of unconventional structures.[5−7] For example, linear-branched block copolymers with multiple short chains tethered on the junction point have been demonstrated to effectively shift phase boundaries and stabilize the Frank−Kasper phase and quasicrystalline phase.[8−11] The advances in synthetic techniques provide great opportunities to program the self-assembly behaviors toward the desired structure and properties.

Simply increasing the branching number is, however, not a viable solution to push the phase boundaries. A recent self-consistent field theory (SCFT) study has revealed that the asymmetry of the phase diagram gradually approaches a limit as the number of branches increases.[12] Meanwhile, the efficiency to synthesize branching polymers is severely reduced due to increasingly large steric hindrance.[13] An alternative modification to the branching architecture is thus necessary to circumvent the limit and effectively enlarge the spherical/cylindrical phase region.[12] Li and co-workers recently proposed a promising approach utilizing miktoarm star block copolymers for obtaining extremely asymmetric phase diagrams.[14,15] This miktoarm star block copolymer x(AB$_1$)B$_2$, composed of xAB$_1$ diblock arms and one B$_2$ homopolymer arm, naturally assumes a radial distribution of B blocks with the tendency of forming spontaneous curvature.[14] Moreover, the synergy between the branched and linear chains effectively releases packing frustration. Kim et al. synthesized this type of block copolymers using polystyrene and polystyrene-*block*-poly(2-vinylpyridine)

Received: July 31, 2023
Revised: September 17, 2023
Accepted: September 22, 2023
Published: October 13, 2023

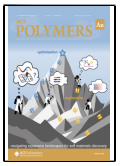

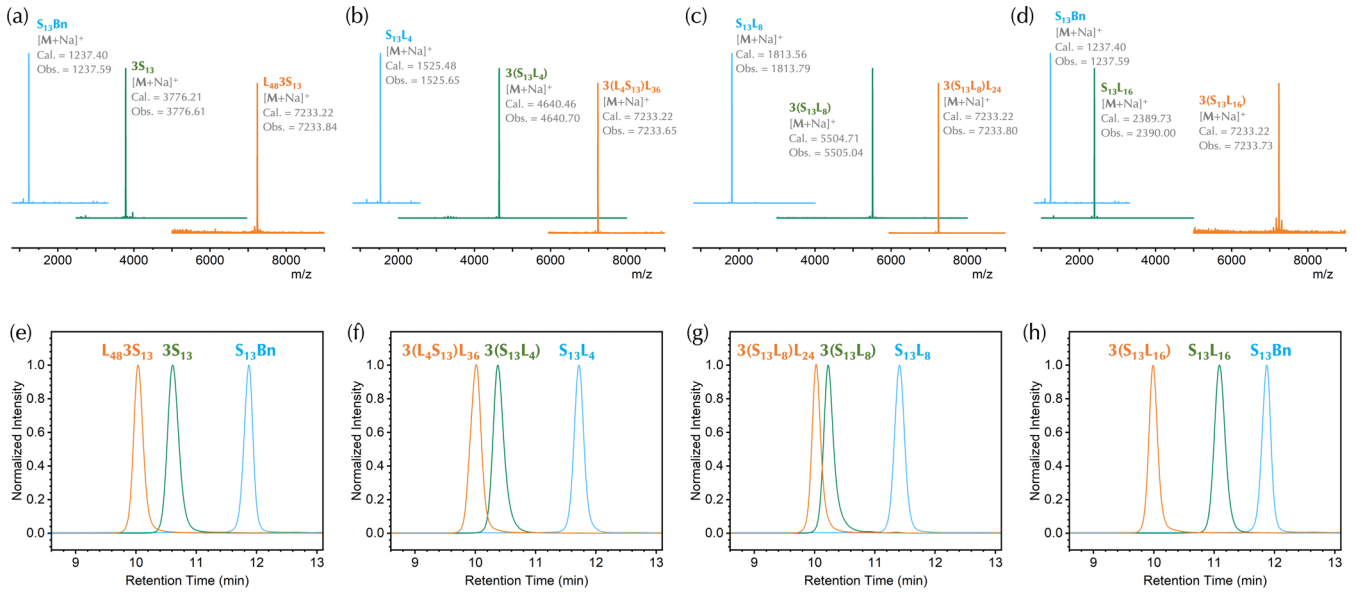

Figure 1. Representative MALDI-ToF MS (a–d) and SEC traces (e–h) of the precursors/intermediates of the isomeric miktoarm star block copolymer with a total n = 48: $3S_{13}L_{48}$ (a, e), $3(S_{13}L_4)L_{36}$ (b, f), $3(S_{13}L_8)L_{24}$ (c, g), and $3(S_{13}L_{16})$ (d, h).

and confirmed a significantly expanded DG phase window at a high volume fraction.[16] An inverted gyroid structure was identified with a f_B = 0.64. Despite the interesting observations, the lack of precise control on the molecular structure impedes a clear understanding on the detailed contribution of the complex architecture to the phase behaviors.

Miktoarm star polymers have long been a topic of intensive research due to their intriguing symmetry-breaking feature.[13,17] The complex chain architecture, however, brings extra challenges in the synthesis and characterization. Though several approaches have been well developed, precise control on the number of arms is still difficult to achieve, and the defects in molecular architecture (such as missing arms) cannot be adequately characterized using conventional techniques such as size exclusion chromatography (SEC). Moreover, the inherent dispersity in multiple arms amplifies compositional fluctuation and significantly influences the structure and properties, covering the essential features. Discrete block copolymers with precise chemical composition and uniform chain length provide an ideal platform for studying the phase behaviors of block copolymers with complex architecture, avoiding the interferences associated with statistical chain length distribution.[18] In this work, we designed and synthesized a series of miktoarm star block copolymers based on oligo-lactic acid (oLA, L) and oligo dimethylsiloxane (oDMS, S). An architectural evolution from the linear-branched block copolymer to the miktoarm star block copolymer to the star-like block copolymer ($3SL \rightarrow 3(SL_1)L_2 \rightarrow 3(SL)$) was achieved by adjusting the relative size of the linear and branched L block. The discrete feature ensures precise regulation of the molecular structure and excludes all molecular uncertainties and defects. The phase behaviors were systematically studied and compared, revealing intriguing details that have not yet been explicitly captured. This study provides deep insights into the critical role of a complex molecular architecture in regulating the formation and evolution of ordered structures.

EXPERIMENTAL SECTION

Syntheses

All of the discrete polymers were prepared following the iterative growth approach. Detailed procedures, schemes, and characterizations can be found in Supporting Information.

Nuclear Magnetic Resonance (NMR)

All ^{1}H NMR spectra were acquired in $CDCl_3$ by using a Bruker 500 MHz NMR spectrometer. The spectra were referenced to the residual solvent peak in $CDCl_3$ at δ 7.26 ppm.

Size Exclusion Chromatography (SEC)

SEC analyses were measured at 40 °C on a Tosoh HLC-8320 instrument equipped with three TSK gel columns (SuperH 2000, SuperH 3000, and SuperH 4000 in series), a double flow type RI detector, and a UV-8320 UV detector using tetrahydrofuran (THF) as eluent. The flow rate was 0.6 mL/min. Data acquisition was performed using EcoSEC software, and molecular weights and molecular weight distributions were calibrated with polystyrene standards (Polymer Laboratories).

Matrix-Assisted Laser Desorption/Ionization Time-of-Flight (MALDI-ToF)

MALDI-ToF mass spectroscopy (MS) was acquired on an UltrafleXtreme MALDI-ToF mass spectrometer (Bruker Daltonics) equipped with a 1 kHz smart beam-II laser. Trans-2-[3-(4-*tert*-butylphenyl)-2-methyl-2-propenylidene]-malononitrile (DCTB, Sigma-Aldrich, > 98%) was used as the matrix and prepared in $CHCl_3$ at a concentration of 20 mg/mL. The cationizing agent sodium trifluoroacetate was prepared in ethanol at a concentration of 10 mg/mL. The matrix and cationizing salt solutions were mixed in a ratio of 10:1 (v/v). All samples were dissolved in $CHCl_3$ at a concentration of 10 mg/mL. The attenuation of the laser was adjusted to minimize undesired polymer fragmentation and maximize the sensitivity.

Small-Angle X-ray Scattering (SAXS)

SAXS experiments were performed on Shanghai Synchrotron Radiation (SSRF), beamline BL16B1. The incident X-ray photon energy was 10 keV; the wavelength of the X-ray was 0.124 nm; the photo 3 flux was 1×10^{11} phs/s. Scattered X-rays were captured on a 2-dimensional Pilatus detector. The instrument was calibrated with diffraction patterns from silver behenate. Different annealing protocols have been applied. In general, samples were heated above T_{ODT} for 10 min on a Linkam hot stage (LTS420) and then annealed at 25 °C. Some samples were also

https://doi.org/10.1021/acspolymersau.3c00017
ACS Polym. Au 2023, 3, 457–465

Scheme 1. Schematic Illustration of the Miktoarm Star Block Copolymers with Varied Molecular Architectures: Linear-Branched (Left), Miktoarm (Middle), and Star-Like (Right)

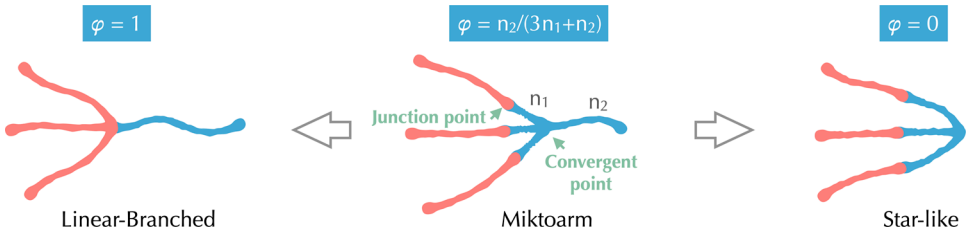

Scheme 2. Chemical Structure of the Arms (a) and Synthetic Route of the Miktoarm Star Block Copolymer $3(S_{13}L_{n1})L_{n2}$ (b)

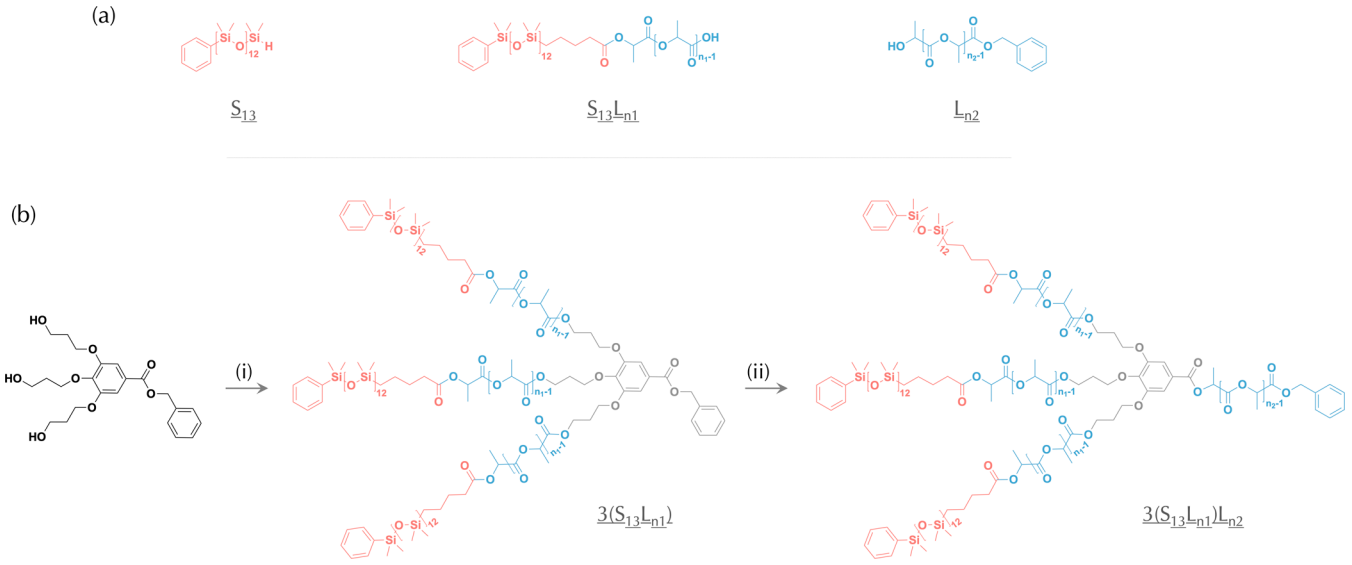

Table 1. Molecular and Structural Characterizations of Discrete Block Copolymers

sample	MW_{calcd} [a]	MW_{obs} [b]	f_L [c]	φ [d]	phase [e]	a (nm) [f]	T_{ODT} [g]
$3S_{13}L_{36}$	6345.98	6368.82	0.41	1	HEX	10.80	140
$3(S_{13}L_4)L_{24}$	6345.98	6368.72	0.41	0.67	A15	18.49[3]	40
$3(S_{13}L_{12})$	6345.98	6368.79	0.41	0	Dis		
$3S_{13}L_{48}$	7210.22	7233.84	0.47	1	HEX	12.60	170
$3(S_{13}L_4)L_{36}$	7210.22	7233.65	0.47	0.75	HEX	10.39	100
$3(S_{13}L_8)L_{24}$	7210.22	7233.80	0.47	0.50	LAM	6.72	25
$3(S_{13}L_{16})$	7210.22	7233.73	0.47	0	LAM	6.82	50
$3S_{13}L_{60}$	8074.47	8097.87	0.53	1	HEX	14.25	200
$3(S_{13}L_4)L_{48}$	8074.47	8097.67	0.53	0.80	HEX	12.21	130
$3(S_{13}L_8)L_{36}$	8074.47	8098.11	0.53	0.60	HEX	10.80	60
$3(S_{13}L_{20})$	8074.47	8098.15	0.53	0	LAM	7.32	80
$3S_{13}L_{72}$	8938.71	8962.30	0.57	1	DG	29.31	230
$3(S_{13}L_4)L_{60}$	8938.71	8962.25	0.57	0.83	HEX	13.68	160
$3(S_{13}L_8)L_{48}$	8938.71	8962.17	0.57	0.67	HEX	12.32	90
$3(S_{13}L_{12})L_{36}$	8938.71	8962.23	0.57	0.5	LAM	7.76	50
$3(S_{13}L_{24})$	8938.71	8962.31	0.57	0	LAM	7.78	80

[a]Overall exact molecular weight, Da. [b]Molecular weight observed by MALDI-ToF MS, $[M + Na]^+$, Da. [c]Volume fraction of oLA block. [d]Architectural parameter, $\varphi = n_2/(3n_1 + n_2)$. [e]Phase, determined by SAXS. [f]Lattice dimensions: interlamellar spacing of LAM, intercolumn distances of HEX, or lattice parameters of DG and A15 phase. [g]Order-to-disorder transition temperature (°C), determined by SAXS. See Supporting Information for detailed calculations.

further annealed at elevated temperatures for additional time (ca. 1 day).

RESULTS AND DISCUSSION

Miktoarm star block copolymers $3(S_{13}L_{n1})L_{n2}$, together with the architectural isomers, were modularly synthesized through a sequential coupling method (Figure 1, where the subscripts refer to the exact number of repeat units). The oLA and oDMS homopolymers, each with a discrete number of repeat units, were first prepared following the iterative growth approach (Schemes S1 and S2).[19−21] Subsequently, the hydrosilyl end of the oDMS chain was converted to a carboxyl group (protected

https://doi.org/10.1021/acspolymersau.3c00017
ACS Polym. Au 2023, 3, 457−465

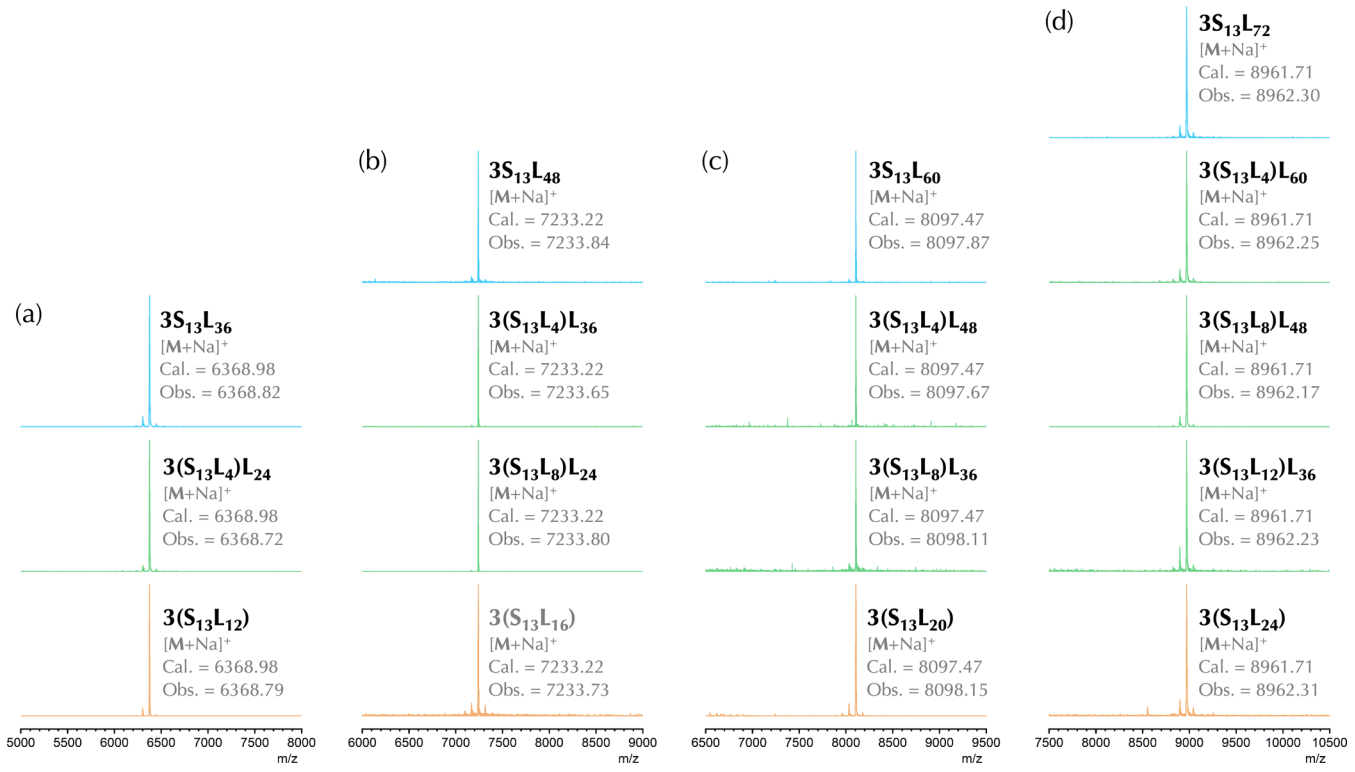

Figure 2. MALDI-ToF MS of the discrete block copolymers with different architectures: n = 36 (a), 48 (b), 60 (c), and 72 (d).

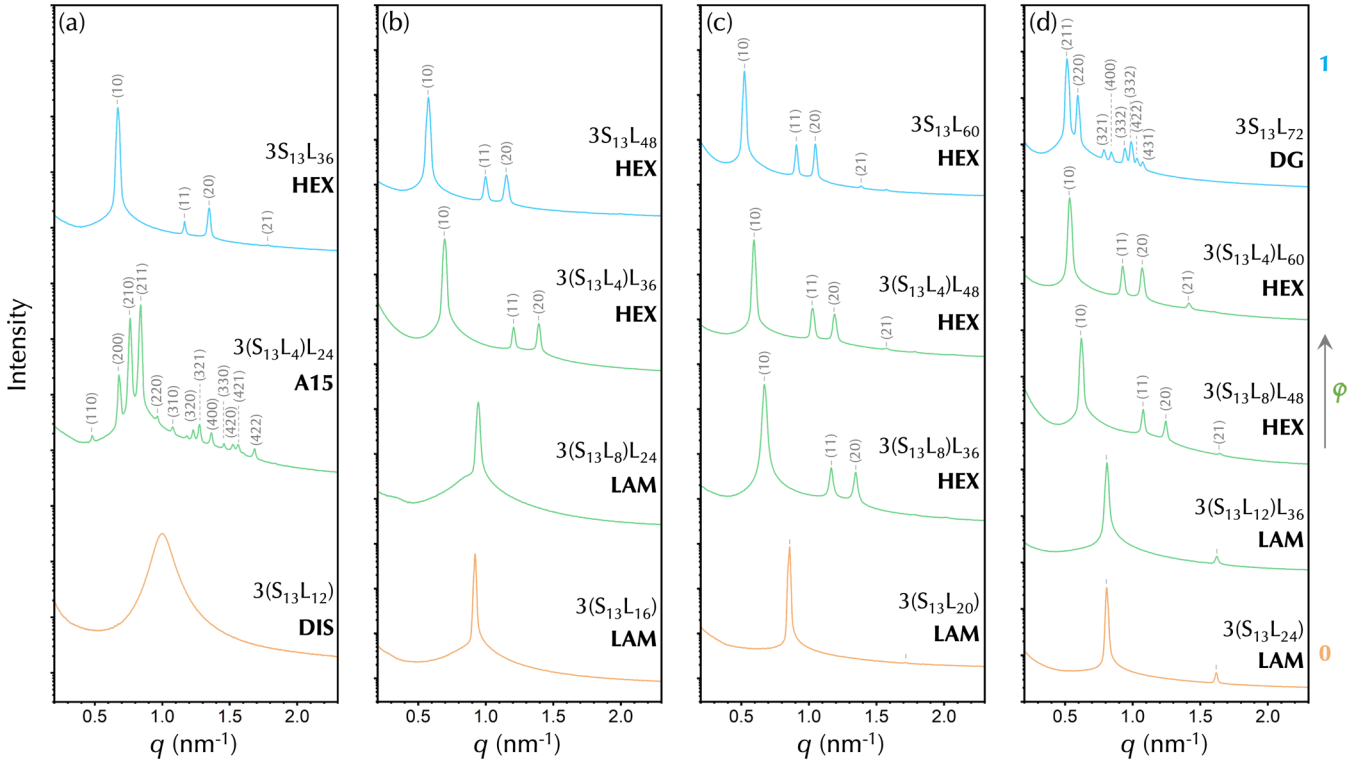

Figure 3. SAXS profiles of the discrete block copolymers with different architectures: n = 36 (a), 48 (b), 60 (c), and 72 (d). Linear-branched block copolymers ($3S_{13}L_n$) are depicted in cyan, star-like block copolymers $3(S_{13}L_n)$ in orange, and the miktoarm star block copolymer in green. Data are shifted vertically for clarity.

by a benzyl group) and conjugated with an oLA block via esterification, yielding an oDMS−oLA block copolymer ($S_{13}L_{n1}$, Scheme S6).[22] An adapter consisting of three hydroxyl groups and one latent carboxyl group (i.e., masked by a benzyl group) was designed for modular chain extension (Scheme S3). Consecutively coupling three oDMS−oLA block copolymers and one oLA homopolymer onto the hydroxyl and carboxylic end yields the designed miktoarm star block copolymer

https://doi.org/10.1021/acspolymersau.3c00017
ACS Polym. Au 2023, 3, 457−465

$3(S_{13}L_{n1})L_{n2}$ (Scheme 2). Meanwhile, the linear-branched block copolymers ($3S_{13}L_n$) with $n_1 = 0$ were prepared by directly installing three oDMS homochains (Schemes S4 and S5). Note that the linear-branched polymers also exhibit a miktoarm architecture consisting of different homopolymer arms. For clarity, the term linear-branched in this study refers specifically to this set of samples (Scheme 1). On the other hand, the star-like counterparts ($3(S_{13}L_n)$) with $n_2 = 0$ were prepared without coupling the linear oLA homopolymer (Scheme S7). To capture the detailed architectural features, a dimensionless parameter $\varphi = n_2/(3n_1 + n_2)$ was introduced, defined as the fraction of the linear oLA chain to the total oLA component (Scheme 1).[15] Accordingly, the miktoarm star block copolymers are reduced to linear-branched copolymers $3S_{13}L_n$ when $\varphi = 1$ or star-like diblock copolymers $3(S_{13}L_n)$ when $\varphi = 0$ (Scheme 2). A summary of the detailed molecular information is provided in Table 1.

The resultant block copolymers were verified by nuclear magnetic resonance (NMR), size exclusion chromatography (SEC), and matrix-assisted laser desorption/ionization time-of-flight mass spectrometry (MALDI-ToF MS). The characterization of the related precursors/intermediates is shown in Figure 1. In general, MALDI-ToF MS shows a single peak with a molecular mass agreeing well with the calculated value, confirming the precise chemical identity and the discrete feature of the block copolymers (Figure 1a–d). The purity of the samples was validated by ^{1}H NMR, in which characteristic resonances from both oDMS and oLA blocks were identified (Figures S1 and S2). Moreover, all of the SEC elution traces are narrow and unimodal, with a clear increase of hydrodynamic volume upon block extension (Figure 1e–h). Interestingly, the star-like block copolymers $3(S_{13}L_n)$ assume a more expanded conformation (a lower retention time) compared to the isomeric linear-branched counterparts (Figure S3), likely due to the architectural differences (3 arms vs 4 arms).

In this study, four sets of isomeric block copolymers with varying overall oLA lengths (n = 36, 48, 60, and 72) were synthesized and studied in parallel (Figure 2). For each set, the isomers have the same composition, differing only in the relative sizes of the linear and branched oLA blocks (n_1 and n_2). The inherent chemical incompatibility between oDMS and oLA blocks drives the phase separation. All specimens were first heated to above the order-to-disorder transition temperature (T_{ODT}) to remove thermal history and then annealed at 40 °C to develop ordered structures. The resultant molecular packings were characterized by using small-angle X-ray scattering (SAXS). Due to the low glass transition temperature, acquiring transmission electron microscopy (TEM) images of these viscous liquid-like samples was rather challenging. Nonetheless, the high-quality SAXS profiles provide convincing evidence to support the proposed nanostructures.

The phase behavior of the linear-branched block copolymer ($3S_{13}L_n$) has been briefly investigated in our earlier studies.[11,23] In this work, three samples with n = 36, 48, and 60 were assembled into the same HEX structure with oLA cylinders embedded in the oDMS matrix (Figure 3a–c, cyan curves). An increase in the intercolumn distance from 10.80 to 12.60 and 14.25 nm was recorded as the chain length increased (Table 1). The lattice dimension a increases as the oLA chain length increases, with an approximate linear correlation. It should be noted that, however, it does not contradict the scaling law (typically $d \sim M^{2/3}$), as these oligomers cannot be depicted by the Gaussian chain model due to the short size and the molecular weight range is too narrow to unravel the overall picture. Further increasing the oLA chain length ($3S_{13}L_{72}$) triggers a transition to the DG phase with two continuous oLA channels, as indicated by a dense forest of scattering peaks with a characteristic ratio of $\sqrt{6}$:$\sqrt{8}$ (Figure 3d). Despite the relatively symmetric composition, the branched architecture induces spontaneous curvature toward the linear oLA domain.[11] As a result, HEX and DG phases emerge instead of the LAM phase, and the HEX/DG phase boundary is significantly deflected to f_L between 0.53 and 0.57.

In contrast, LAM structure consisting of alternating oLA and oDMS layers were observed in the star-like block copolymers $3(S_{13}L_n)$ bearing three linear block arms (except the sample $3(S_{13}L_{12})$ that remain disordered due to insufficient segregation strength; brown curves in Figure 3). The lamellar periodicity (d) increases as n increases, from 6.82 nm (n = 16) to 7.32 nm (n = 20) and to 7.78 nm (n = 24) (Table 1). In general, the star-like block copolymers behave like the constituent AB diblock copolymer. For example, linear $S_{13}L_{24}$ forms a similar lamellar structure as that of $3(S_{13}L_{24})$.[24] A slight yet continuous expansion of domain size was recorded as the number of arms increases, as exemplified by a comparison between $S_{13}L_{24}$ (d = 6.75 nm), $L_{24}S_{24}L_{24}$ (d = 7.39 nm), and $3(S_{13}L_{24})$ (d = 7.78 nm).[24] Additionally, increasing the number of arms also enhances the thermal stability of the star-like block copolymers. The order-to-disorder transition of $3(S_{13}L_{24})$ occurs at T_{ODT} = 80 °C, as revealed by the temperature-dependent SAXS experiments (Figure S8). The linear counterpart $S_{13}L_{24}$, on the other hand, shows a significantly lower T_{ODT} at 35 °C.[24] Compared with the linear AB diblock counterpart, covalently bonding onto a junction point introduces additional constraints to depress translational freedom, reducing the entropy penalty upon the formation of ordered structures. From a different perspective, the star-like block copolymers are much more difficult to pull out from the assembled motifs due to the existence of multiple anchoring sites, and thus, the structure remains intact up to a higher temperature. A theoretical study by Matsen has demonstrated that the increasing branching arms would reduce the critical segregation strength (χN) at the order–disorder transition without significantly distorting the phase diagram.[5] Indeed, the star-like architecture produces a notably less effect on the phase diagram than that of linear-branched block copolymers (Figure 3).

The phase behaviors of the $3(S_{13}L_{n1})L_{n2}$ miktoarm star block copolymer display appreciable differences from both the linear-branched and star-like references discussed above (Figure 3, green curves). We first look at the block copolymers with the lowest volume fraction in this study (n = 36, f_L = 0.41; Figure 3a). In contrast to their linear-branched counterpart that adopts the HEX packing ($3S_{13}L_{36}$, $\varphi = 1$), the scattering profile of the sample $3(S_{13}L_4)L_{24}$ (φ = 0.67) exhibits a dense array of peaks, which can be assigned to a Frank–Kasper A15 phase with a cubic unit cell ($a = b = c$ = 18.49 nm). The Frank–Kasper phases are a family of low-symmetry spherical phases composed of polyhedral motifs with varying shapes, sizes, and coordination numbers.[25−29] Typically, the formation of the Frank–Kasper phase in block copolymers requires sufficiently large conformational asymmetry, originating from either difference in Kuhn length or asymmetric architecture ($\varepsilon = xb_B/b_A$, where b is the statistical segment length of two unlike blocks).[9,30,31] Note that the maximum volume fraction of the A15 phase attained by a four-arm linear-branched block copolymer was identified to be f_L = 0.35 ($4S_{13}L_{40}$).[11] It is interesting that the existence of a

https://doi.org/10.1021/acspolymersau.3c00017
ACS Polym. Au 2023, 3, 457−465

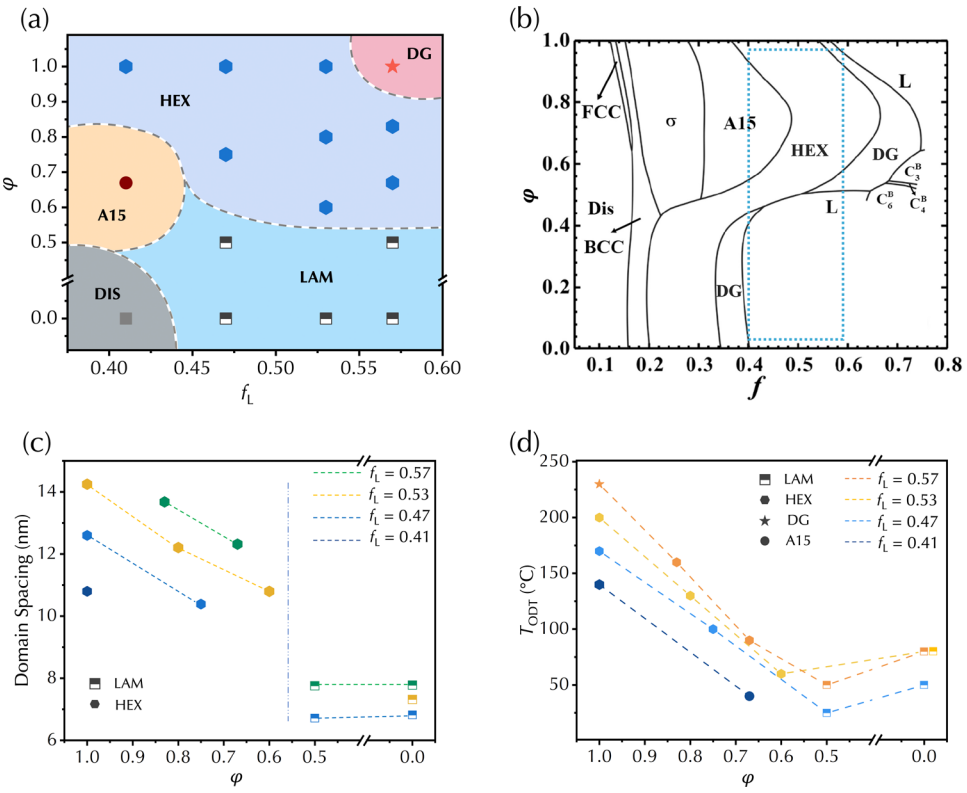

Figure 4. (a, b) Phase portrait of the miktoarm star block copolymers (a), which agrees well with the calculated results by Li and co-workers (b).[15] (c, d) Variation of domain spacing (c) and order-to-disorder transition temperature (T_{ODT}, d) as the molecular architecture changes. Panel (b) adapted with permission from ref 15. Copyright 2020 American Chemical Society.

short-branched oLA chain further deflects the phase boundary to an exceedingly large volume fraction.

On the other hand, the sample set with the largest volume fraction (n = 72, f_L = 0.57) shows also interesting transitions as the architecture changes (Figure 3d). Compared with the linear-branched counterpart ($3S_{13}L_{72}$, φ = 1) forming a DG phase with oLA channels embedding in the oDMS matrix, the isomers $3(S_{13}L_4)L_{60}$ (φ = 0.83) and $3(S_{13}L_8)L_{48}$ (φ = 0.67) adopt HEX molecular packing, with lattice dimension decreases from d = 13.68 to d = 12.62 nm. Further decreasing φ leads to a phase transition toward the LAM structure ($3(S_{13}L_{12})L_{36}$, φ = 0.5), similar to the star-like block copolymer $3(S_{13}L_{24})$ with φ = 0. The same tendency (i.e., from HEX to LAM) was observed in the other sets of samples (n = 48 and 60, Figure 3b,c).

The chain architecture also exerts a profound influence on the stability of the assembled structures. Direct evidence comes from the block copolymers with n = 36. The T_{ODT} of the linear-branched block copolymer ($3S_{13}L_{36}$) was found to be around 140 °C (Figure S5), whereas the star-like counterpart $3(S_{13}L_{12})$ remains disordered even at room temperature (Figure 3a). The order-to-disorder transition temperature (T_{ODT}) of the isomers with varying φ values was then carefully measured and compared using temperature-dependent small-angle X-ray scattering (SAXS). Take the sample set with n = 72 as an example. The linear-branched block copolymer $3S_{13}L_{72}$ exhibits a remarkably high T_{ODT} of 230 °C. As φ decreases, the transition temperature continuously drops, reaching a T_{ODT} of 60 °C in the case $3(S_{13}L_{12})L_{36}$ (Figure S8). Interestingly, a slight increase of T_{ODT} was recorded in the star-like counterpart $3(S_{13}L_{24})$ (T_{ODT} = 80 °C). Similar behaviors were observed in parallel across other groups of block copolymers (Figure 4d).

Figure 4a provides an overview of the obtained phase portrait with varying composition and symmetry, highlighting the profound influence of the molecular architecture on phase behaviors. If viewing horizontally, we focus on the compositional variation. In general, transitions from a phase with high curvature toward those with lower curvature were recorded as f_{LA} increases for a given φ (e.g., HEX → DG at φ = 1; A15 → HEX at φ = 0.7). Along the perpendicular direction, all of the isomers have the same composition. The assembled structures are sensitive to architectural variation, and the phase boundaries are significantly deflected. It should be noted that the degree of deflection is not monotonically changed. Take the HEX/DG phase boundary as an example. This boundary locates at $f_L \approx$ 0.55 in the linear-branched block copolymer with φ = 1. It is well-known that branched architecture favors interfacial curvature toward the linear component, and thus, the HEX phase appears at a relatively higher volume fraction compared to that of AB linear diblock copolymers. Interestingly, the existence of short branching *o*LA chains in the miktoarm star block copolymers ($0.5 < \varphi < 1$) pushes the HEX/DG phase boundary to an even higher volume fraction of oLA ($f_L > 0.57$). On the other hand, this boundary shifts to a much lower volume fraction ($f_L < 0.47$) when the branched oLA chains are sufficiently long ($\varphi < 0.5$), similar to the AB diblock copolymer. Li and co-workers have constructed a phase diagram of $3(AB_1)B_2$ as a function of volume fraction (f) and structural parameter (φ) based on SCFT computation (Figure 4b).[15] Our experimental observations are in excellent agreement with the calculated results, exhibiting the same features including the non-monotonic deflection of phase boundaries, the appearance of A15 and DG phases, and the transition from the HEX to LAM phase with decreasing φ.

https://doi.org/10.1021/acspolymersau.3c00017
ACS Polym. Au 2023, 3, 457−465

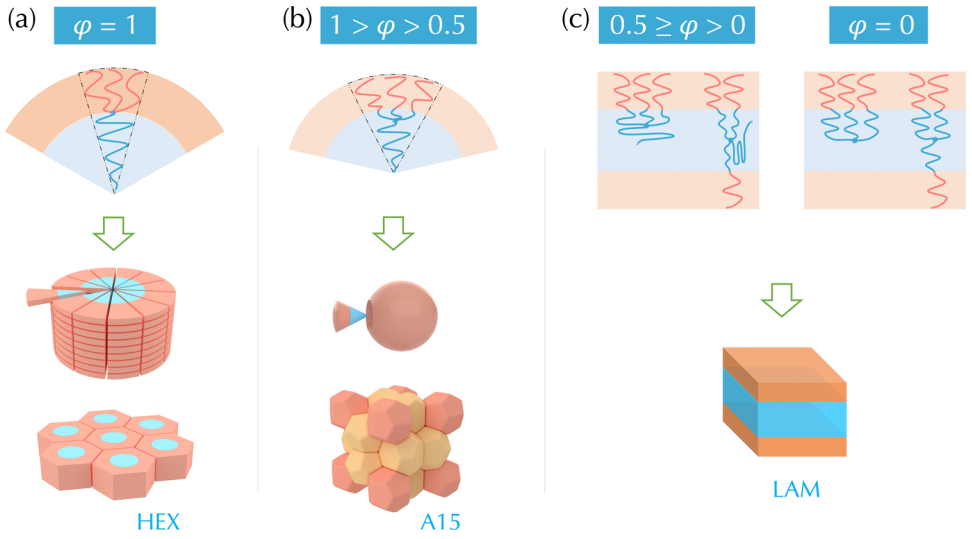

Figure 5. Schematic illustration of the molecular packing with varied φ. The block copolymers assume fan-like (a), cone-like (b), or flat (c) shapes (upper), which further aggregate into cylindrical (a), spherical (b), or layer-like (c) motifs for further assembly (lower).

It has long been recognized that the self-assembly behaviors of the simplest AB linear diblock block depend mainly on three molecular variables: overall chain length (N), volume fraction (f), and Flory–Huggins interaction parameter (χ). The detailed influence of molecular symmetry is, however, not explicitly captured by the classic phase principles. All of the isomeric block copolymers have nominally the same composition (f) and segregation strength (χN). Moreover, they are also supposed to have the same conformational asymmetry (ε) based on the definition.[9,32] Nevertheless, it is evident that the location of the junction point(s) between the dissimilar blocks profoundly influences the underlying molecular packing. For the linear-branched block copolymers with φ = 1, the junction point coincides with the convergent point, and the multiple branching blocks assume a cone shape to accommodate the increasing volume along the radial direction (toward the outside, Figure 5a). Samples $3(S_{13}L_{n1})L_{n2}$ with a short-branched oLA ($1 \geq \varphi \geq 0.5$), on the other hand, adopt a similar cone-like molecular shape, as the distance between the junction points and the convergent point is too short to form a bridge configuration (Figure 5b). The branched blocks and the linear block assemble into a core–shell structure, wherein the former resides in the outer layer, while the latter occupies the inner region. The existence of three short branching chains prompts the spontaneous curvature, effectively alleviating the stretching of the oLA component. The increased wedge angle reduces the intercolumnar distance and even facilitates a transition from a cylindrical phase to a spherical phase. The boundary is largely deflected when the linear and branched oLA blocks form a radial distribution, with the curvature commensurate with the growing trend of the volume along the radial direction. When the length of the branching oLA further increases (i.e., $\varphi < 0.5$), on the other hand, the demand of the junction points in the same interface is largely relaxed. Both loop and bridge configurations become accessible. The formation of a bridge configuration allows the oDMS blocks to be distributed in the neighboring domains. As a result, the block copolymers resemble the feature of AB linear diblock copolymers, forming the LAM phase at a symmetric volume fraction (Figure 5c).

The difference in phase stability is also closely related to the location of the junction points, which not only influences the interfacial area (enthalpic contribution) but also determines the ratio between the bridge and loop configurations (entropic contribution) upon phase separation. For a linear-branched block copolymer, all the oDMS blocks must be in the same domain (Figure 5a). As φ decreases, the junction point(s) between the immiscible blocks shifts from the convergent point to the three branched chains, leading to a significant increase in the interfacial area and a concomitant decrease of T_{ODT} (Figure 5b). Gradually moving the junction points along the branched chains leads to an increasing conformational entropy penalty to confine three oDMS blocks in the same domain and thus results in a continuous drop of phase stability. On the other hand, as the branching chains are sufficiently long (e.g., $\varphi < 0.5$), the existence of the bridge configuration would release the conformational entropy loss (due to stretching) and increase the translational entropy as the junction point can be distributed to different interfaces.[14] The entropic gain thus leads to an enhanced phase stability. The non-monotonic variation of T_{ODT} observed in our study is in line with the χN_{ODT} predicted in the computational work by Li and co-workers employing the random-phase approximation (RPA).[15]

CONCLUSIONS

In summary, we conducted a detailed investigation of the critical role of molecular architecture in phase behaviors using a library of precisely defined block copolymers. The molecular architecture was meticulously regulated by tuning the relative chain length of the linear and branched blocks while the overall composition remains unchanged. The phase behaviors were examined and compared by tuning the volume fraction and architectural parameters. Compared with the linear-branched block copolymers, miktoarm star block copolymers with a radial distribution of the minority component can effectively release the packing frustration and stabilize the A15 and HEX phases at a higher volume fraction. With further increasing the branched oLA chains, the architectural constraints were gradually relaxed, and the miktoarm star block copolymer behaves like linear block copolymers. The precise feature eliminates the interferences from molecular uncertainties such as chain length dispersity and missing branched arms, shedding light on the phase behavior of block copolymers possessing complex architectures.

https://doi.org/10.1021/acspolymersau.3c00017
ACS Polym. Au 2023, 3, 457–465

■ ASSOCIATED CONTENT

Supporting Information

The Supporting Information is available free of charge at https://pubs.acs.org/doi/10.1021/acspolymersau.3c00017.

Materials and characterization details; experimental procedures; and additional characterizations (PDF)

■ AUTHOR INFORMATION

Corresponding Authors

Rui Tan − *College of Chemistry, Chemical Engineering and Materials Science, Soochow University, Suzhou 215123, China*; Email: ruitan@suda.edu.cn

Xue-Hui Dong − *South China Advanced Institute for Soft Matter Science and Technology, School of Emergent Soft Matter, South China University of Technology, Guangzhou 510640, China; Guangdong Provincial Key Laboratory of Functional and Intelligent Hybrid Materials and Devices, South China University of Technology, Guangzhou 510640, China*; orcid.org/0000-0002-6395-3103; Email: xdong@scut.edu.cn

Authors

Zhuang Ma − *South China Advanced Institute for Soft Matter Science and Technology, School of Emergent Soft Matter, South China University of Technology, Guangzhou 510640, China*

Zhongguo Liu − *South China Advanced Institute for Soft Matter Science and Technology, School of Emergent Soft Matter, South China University of Technology, Guangzhou 510640, China*

Tianyu Zheng − *South China Advanced Institute for Soft Matter Science and Technology, School of Emergent Soft Matter, South China University of Technology, Guangzhou 510640, China*

Zhanhui Gan − *South China Advanced Institute for Soft Matter Science and Technology, School of Emergent Soft Matter, South China University of Technology, Guangzhou 510640, China*; orcid.org/0000-0002-9646-5747

Complete contact information is available at: https://pubs.acs.org/10.1021/acspolymersau.3c00017

Author Contributions

CRediT: **Zhuang Ma** investigation, writing-original draft; **Zhongguo Liu** investigation; **Tianyu Zheng** investigation; **Zhanhui Gan** investigation; **Rui Tan** supervision, writing-review & editing; **Xue-Hui Dong** conceptualization, funding acquisition, supervision, writing-review & editing.

Notes

The authors declare no competing financial interest.

■ ACKNOWLEDGMENTS

This work was supported by the National Natural Science Foundation of China (22273026), the Recruitment Program of Guangdong (2016ZT06C322), the Research Funds from State and Local Joint Engineering Laboratory for Novel Functional Polymeric Materials, Soochow University (SDGC2109), and the 111 Project (B18023). The authors thank the staff of Beamline BL16B1 at the Shanghai Synchrotron Radiation Facility (SSRF) for assistance with the SAXS experiments.

■ REFERENCES

(1) Bates, F. S. Polymer-Polymer Phase Behavior. *Science* **1991**, *251* (4996), 898−905.

(2) Leibler, L. Theory of Microphase Separation in Block Copolymers. *Macromolecules* **1980**, *13* (6), 1602−1617.

(3) Matsen, M. W.; Bates, F. S. Unifying Weak- and Strong-Segregation Block Copolymer Theories. *Macromolecules* **1996**, *29* (4), 1091−1098.

(4) Matsen, M. W.; Bates, F. S. Origins of Complex Self-Assembly in Block Copolymers. *Macromolecules* **1996**, *29* (23), 7641−7644.

(5) Matsen, M. W. Effect of Architecture on the Phase Behavior of AB-Type Block Copolymer Melts. *Macromolecules* **2012**, *45* (4), 2161−2165.

(6) Bates, F. S.; Hillmyer, M. A.; Lodge, T. P.; Bates, C. M.; Delaney, K. T.; Fredrickson, G. H. Multiblock Polymers: Panacea or Pandora's Box? *Science* **2012**, *336* (6080), 434−440.

(7) Polymeropoulos, G.; Zapsas, G.; Ntetsikas, K.; Bilalis, P.; Gnanou, Y.; Hadjichristidis, N. 50th Anniversary Perspective: Polymers with Complex Architectures. *Macromolecules* **2017**, *50* (4), 1253−1290.

(8) Grason, G. M. The Packing of Soft Materials: Molecular Asymmetry, Geometric Frustration and Optimal Lattices in Block Copolymer Melts. *Phys. Rep.* **2006**, *433* (1), 1−64.

(9) Xie, N.; Li, W.; Qiu, F.; Shi, A.-C. σ Phase Formed in Conformationally Asymmetric AB-Type Block Copolymers. *ACS Macro Lett.* **2014**, *3* (9), 906−910.

(10) Bates, M. W.; Barbon, S. M.; Levi, A. E.; Lewis, R. M.; Beech, H. K.; Vonk, K. M.; Zhang, C.; Fredrickson, G. H.; Hawker, C. J.; Bates, C. M. Synthesis and Self-Assembly of ABn Miktoarm Star Polymers. *ACS Macro Lett.* **2020**, *9* (3), 396−403.

(11) Sun, Y.; Tan, R.; Ma, Z.; Gan, Z.; Li, G.; Zhou, D.; Shao, Y.; Zhang, W.-B.; Zhang, R.; Dong, X.-H. Discrete Block Copolymers with Diverse Architectures: Resolving Complex Spherical Phases with One Monomer Resolution. *ACS Cent. Sci.* **2020**, *6* (8), 1386−1393.

(12) Qiang, Y.; Li, W.; Shi, A.-C. Stabilizing Phases of Block Copolymers with Gigantic Spheres via Designed Chain Architectures. *ACS Macro Lett.* **2020**, *9* (5), 668−673.

(13) Liu, M.; Blankenship, J. R.; Levi, A. E.; Fu, Q.; Hudson, Z. M.; Bates, C. M. Miktoarm Star Polymers: Synthesis and Applications. *Chem. Mater.* **2022**, *34* (14), 6188−6209.

(14) Gao, Y.; Deng, H.; Li, W.; Qiu, F.; Shi, A.-C. Formation of Nonclassical Ordered Phases of AB-Type Multiarm Block Copolymers. *Phys. Rev. Lett.* **2016**, *116* (6), No. 068304.

(15) Li, C.; Dong, Q.; Li, W. Largely Tunable Asymmetry of Phase Diagrams of A(AB)n Miktoarm Star Copolymer. *Macromolecules* **2020**, *53* (24), 10907−10917.

(16) Seo, Y.; Woo, D.; Li, L.; Li, W.; Kim, J. K. Phase Behavior of PS-(PS-b-P2VP)3 Miktoarm Star Copolymer. *Macromolecules* **2021**, *54* (17), 7822−7829.

(17) Khanna, K.; Varshney, S.; Kakkar, A. Miktoarm Star Polymers: Advances in Synthesis, Self-Assembly, and Applications. *Polym. Chem.* **2010**, *1* (8), 1171−1185.

(18) van Genabeek, B.; Lamers, B. A. G.; Hawker, C. J.; Meijer, E. W.; Gutekunst, W. R.; Schmidt, B. V. K. J. Properties and Applications of Precision Oligomer Materials; Where Organic and Polymer Chemistry Join Forces. *J. Polym. Sci.* **2021**, *59* (5), 373−403.

(19) Takizawa, K.; Nulwala, H.; Hu, J.; Yoshinaga, K.; Hawker, C. J. Molecularly Defined (L)-Lactic Acid Oligomers and Polymers: Synthesis and Characterization. *J. Polym. Sci., Part A: Polym. Chem.* **2008**, *46* (18), 5977−5990.

(20) van Genabeek, B.; de Waal, B. F. M.; Gosens, M. M. J.; Pitet, L. M.; Palmans, A. R. A.; Meijer, E. W. Synthesis and Self-Assembly of Discrete Dimethylsiloxane−Lactic Acid Diblock Co-Oligomers: The Dononacontamer and Its Shorter Homologues. *J. Am. Chem. Soc.* **2016**, *138* (12), 4210−4218.

(21) Tan, R.; Zhou, D.; Liu, B.; Sun, Y.; Liu, X.; Ma, Z.; Kong, D.; He, J.; Zhang, Z.; Dong, X.-H. Precise Modulation of Molecular Weight Distribution for Structural Engineering. *Chem. Sci.* **2019**, *10* (46), 10698−10705.

(22) Sun, Y.; Tan, R.; Ma, Z.; Zhou, D.; Li, J.; Kong, D.; Dong, X.-H. Quantify the Contribution of Chain Length Heterogeneity on Block Copolymer Self-Assembly. *Giant* **2020**, *4*, No. 100037.
(23) Ma, Z.; Tan, R.; Gan, Z.; Zhou, D.; Yang, Y.; Zhang, W.; Dong, X.-H. Modulation of the Complex Spherical Packings through Rationally Doping a Discrete Homopolymer into a Discrete Block Copolymer: A Quantitative Study. *Macromolecules* **2022**, *55* (11), 4331−4340.
(24) Cai, D.; Li, J.; Ma, Z.; Gan, Z.; Shao, Y.; Xing, Q.; Tan, R.; Dong, X.-H. Effect of Molecular Architecture and Symmetry on Self-Assembly: A Quantitative Revisit Using Discrete ABA Triblock Copolymers. *ACS Macro Lett.* **2022**, *11*, 555−561.
(25) Lee, S.; Bluemle, M. J.; Bates, F. S. Discovery of a Frank-Kasper σ Phase in Sphere-Forming Block Copolymer Melts. *Science* **2010**, *330* (6002), 349−353.
(26) Gillard, T. M.; Lee, S.; Bates, F. S. Dodecagonal Quasicrystalline Order in a Diblock Copolymer Melt. *Proc. Natl. Acad. Sci. U.S.A.* **2016**, *113* (19), 5167−5172.
(27) Kim, K.; Schulze, M. W.; Arora, A.; Lewis, R. M.; Hillmyer, M. A.; Dorfman, K. D.; Bates, F. S. Thermal Processing of Diblock Copolymer Melts Mimics Metallurgy. *Science* **2017**, *356* (6337), 520−523.
(28) Bates, M. W.; Lequieu, J.; Barbon, S. M.; Lewis, R. M.; Delaney, K. T.; Anastasaki, A.; Hawker, C. J.; Fredrickson, G. H.; Bates, C. M. Stability of the A15 Phase in Diblock Copolymer Melts. *Proc. Natl. Acad. Sci. U.S.A.* **2019**, *116* (27), 13194−13199.
(29) Dorfman, K. D. Frank−Kasper Phases in Block Polymers. *Macromolecules* **2021**, *54* (22), 10251−10270.
(30) Lee, S.; Leighton, C.; Bates, F. S. Sphericity and Symmetry Breaking in the Formation of Frank−Kasper Phases from One Component Materials. *Proc. Natl. Acad. Sci. U.S.A.* **2014**, *111* (50), 17723−17731.
(31) Reddy, A.; Buckley, M. B.; Arora, A.; Bates, F. S.; Dorfman, K. D.; Grason, G. M. Stable Frank−Kasper Phases of Self-Assembled, Soft Matter Spheres. *Proc. Natl. Acad. Sci. U.S.A.* **2018**, *115* (41), 10233−10238.
(32) Milner, S. T. Chain Architecture and Asymmetry in Copolymer Microphases. *Macromolecules* **1994**, *27* (8), 2333−2335.

https://doi.org/10.1021/acspolymersau.3c00017
ACS Polym. Au 2023, 3, 457−465